doi:10.1038/nature10398

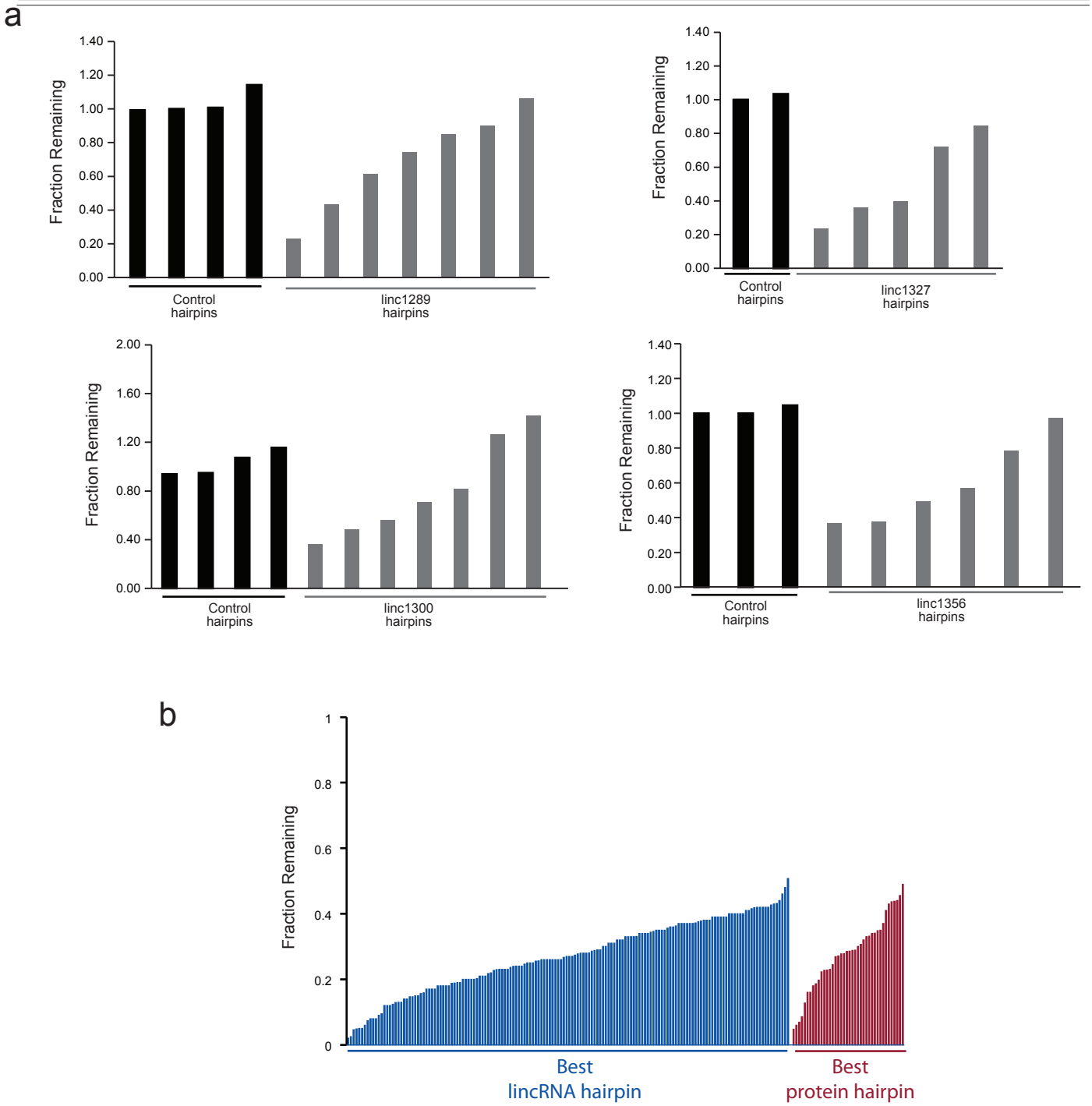

Supplemental Figure 1. Target knockdown levels for lincRNA and Protein-coding hairpins. (a) Fraction expression levels remaining of a lincRNA after infection with negative control hairpins (black bars) and distinct hairpins targeting the same lincRNA (grey) are shown for 4 randomly selected lincRNAs. The distinct hairpins are displayed in sorted order from best knockdown to worst. (b) The best hairpin targeting each lincRNA (blue) and protein-coding gene (red) are shown along with the fraction of the target gene remaining after knockdown.

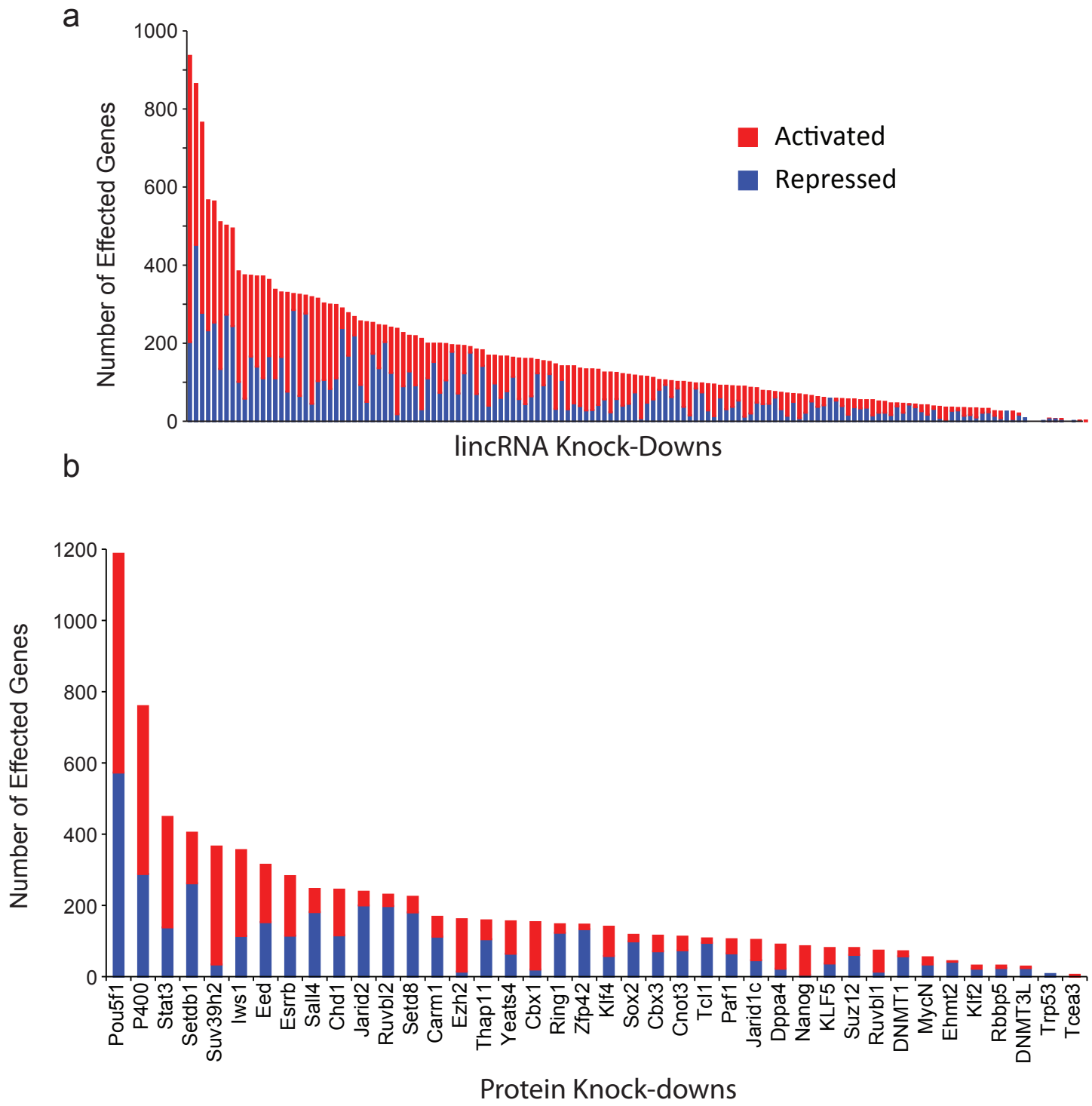

Supplemental Figure 2. Genes affected by knockdown of lincRNA and Protein-coding genes. (a) The total number of genes significantly affected upon knockdown of a lincRNA. The number of activated genes (red) and repressed genes (blue) for each lincRNA knockdown is indicated. (b) The total number of affected genes, activated (red) and repressed (blue), upon knockdown of protein-coding gene controls.

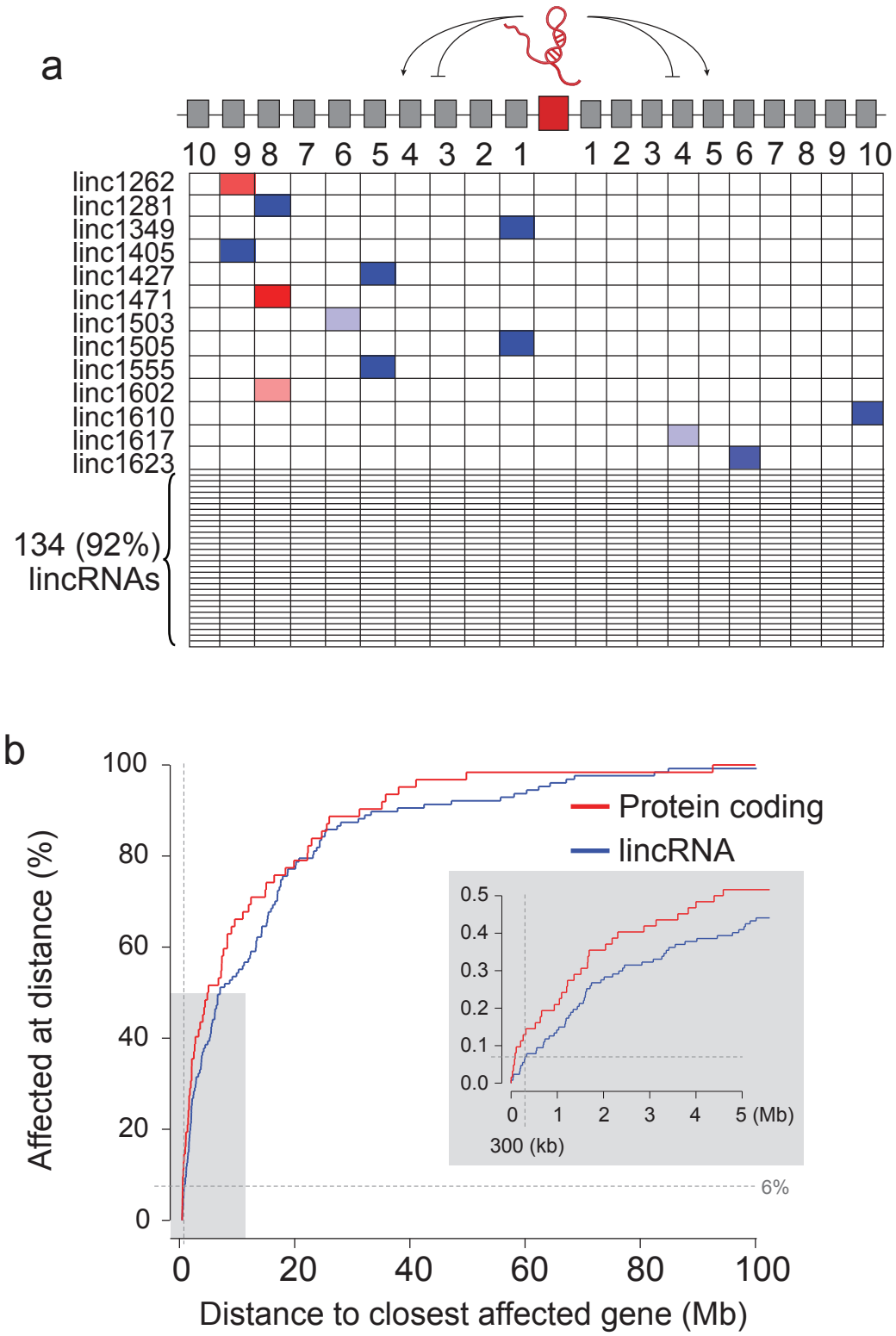

Supplemental Figure 3. lincRNA knockdown effects on neighbouring gene expression. (a) Effects of knockdown of 13 lincRNAs on 10 neighbour genes on each side (blue-downregulation, red-upregulation). For the remaining 134 lincRNA genes, no neighbouring genes are affected. (b) Distance to the closest affected gene upon knockdown of a lincRNA (blue) or protein-coding gene (red). Grey Inset: A close-up of the region from 0–5 Mb. The dashed line represents a distance of 300 kb in both panels.

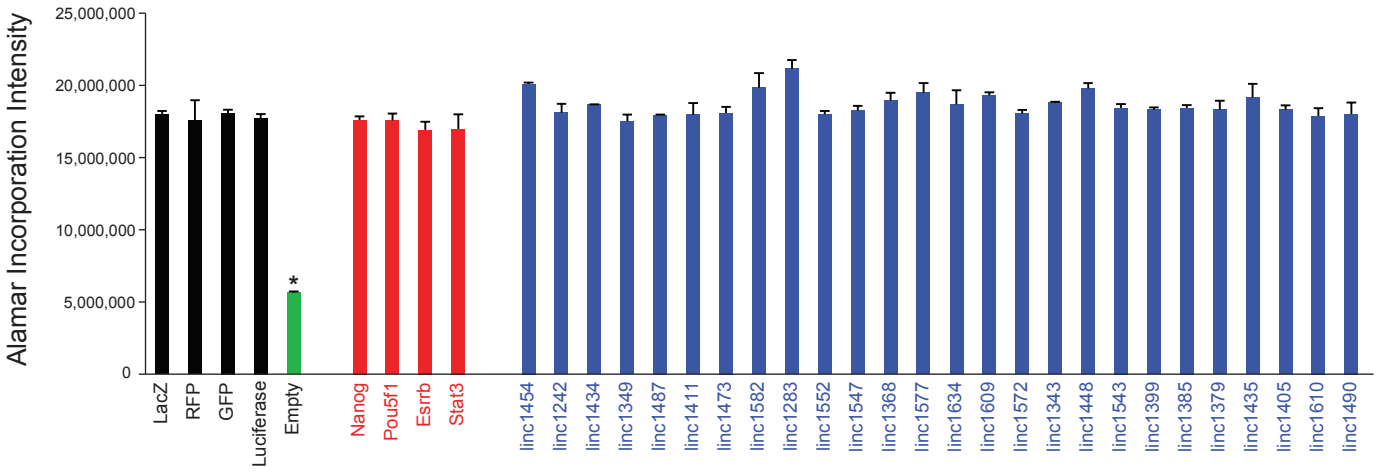

Supplemental Figure 4. lincRNA knockdowns that affect Nanog-Luciferase levels do not affect cell viability. Alamar blue incorporation was measured in Nanog-Luciferase cells infected with control hairpins (black), empty vector controls (green), protein-coding genes (red), and lincRNAs affecting Nanog-Luciferase levels (blue). The ordering of the samples relate to the ordering in Figure 2b. Significant reductions in Alamar incorporation ($p<0.05$) compared to the negative controls are marked with an asterisks.

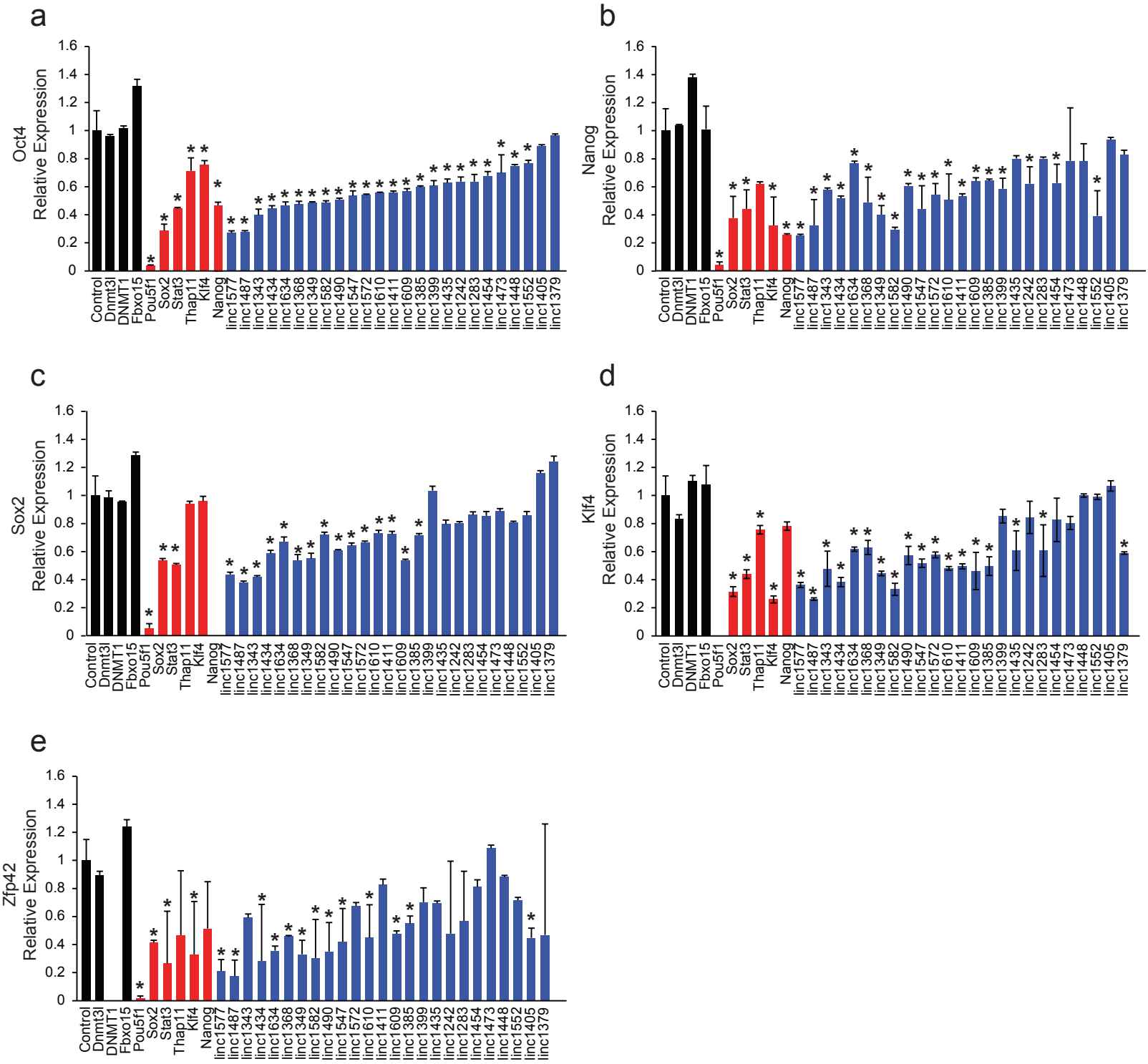

Supplemental Figure 5. lincRNA knockdowns affect mRNA expression of pluripotency markers. (a) The mRNA expression levels assayed by qPCR of (a) Oct4, (b) Nanog, (c) Sox2, (d) Klf4, and (e) Zfp42 after knockdown of negative controls and proteins that do not affect pluripotency (black), known protein-coding regulators of pluripotency (red), and lincRNA genes (blue). Error bars are the standard error across biological replicates. Asterisks represent effects significant at a $p<0.01$ level compared to the negative control hairpins.

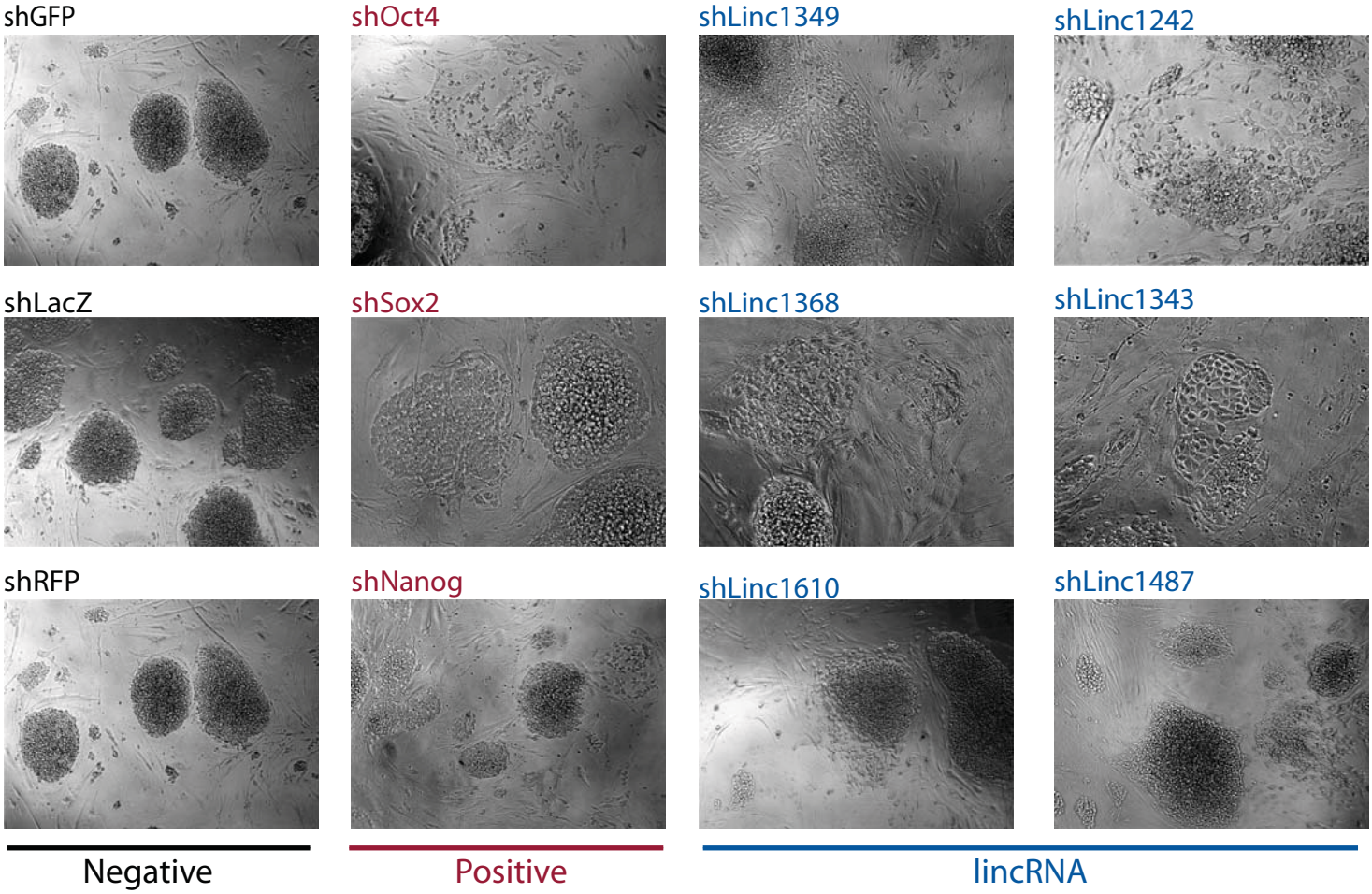

Supplemental Figure 6. lincRNA knockdowns affect ESC morphology. Images of ESCs are shown after RNAi knockdowns. First column (black line) shows negative control hairpins targeting GFP, RFP, and Luciferase. Second column (red line) shows positive control hairpins targeting Oct4, Nanog, and Sox2. Third and fourth column (blue line) shows hairpins targeting lincRNA genes.

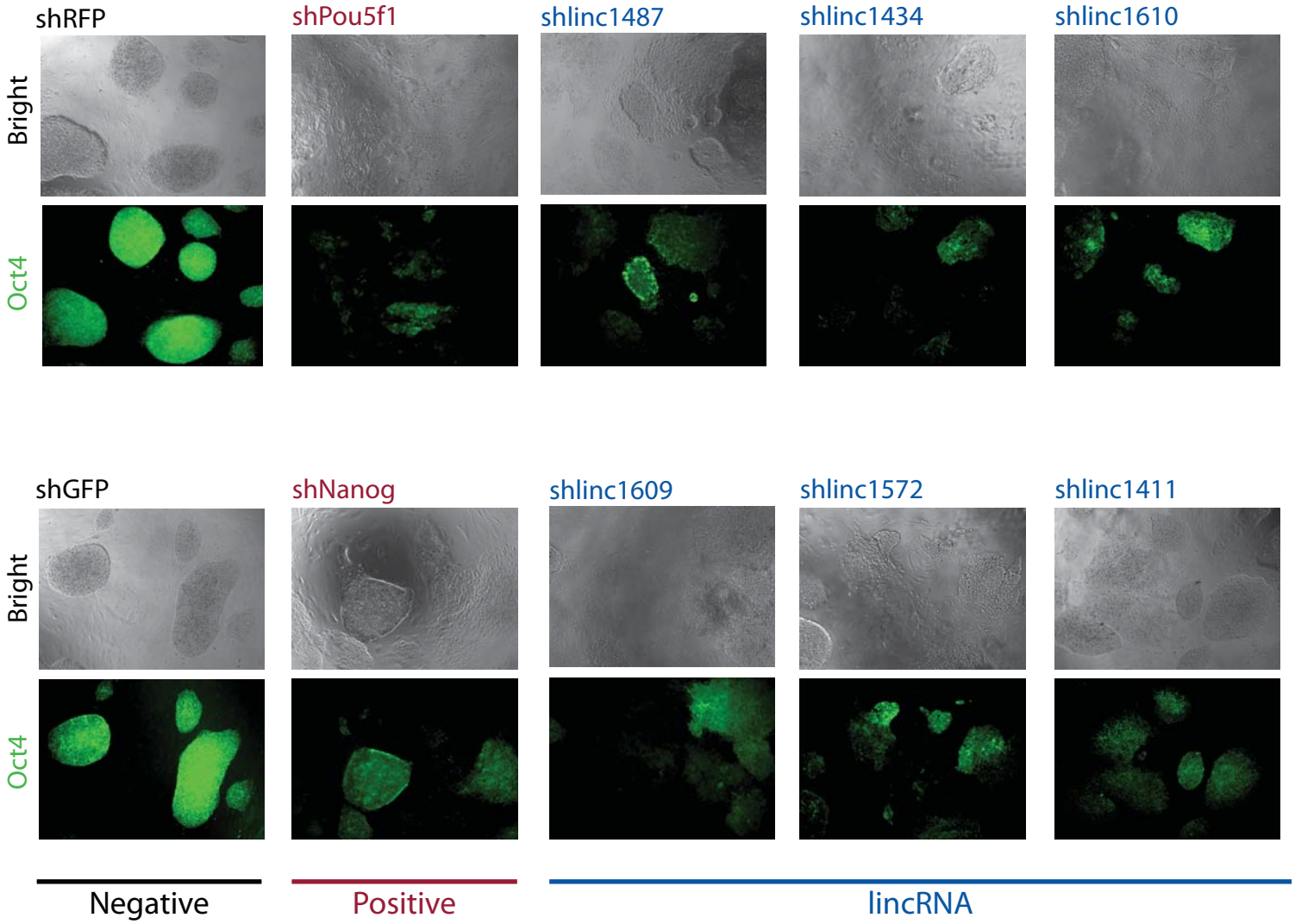

Supplemental Figure 7. lincRNA knockdowns cause a reduction of Oct4 levels. Morphology of ESCs and immunofluorescence staining of Oct4 for negative control hairpins (black line), hairpins targeting protein-coding controls (red line), and hairpins targeting lincRNAs (blue line). The first row of each panel shows bright field images of infected ESCs and the second row shows immunofluorescence staining of the Oct4 protein levels.

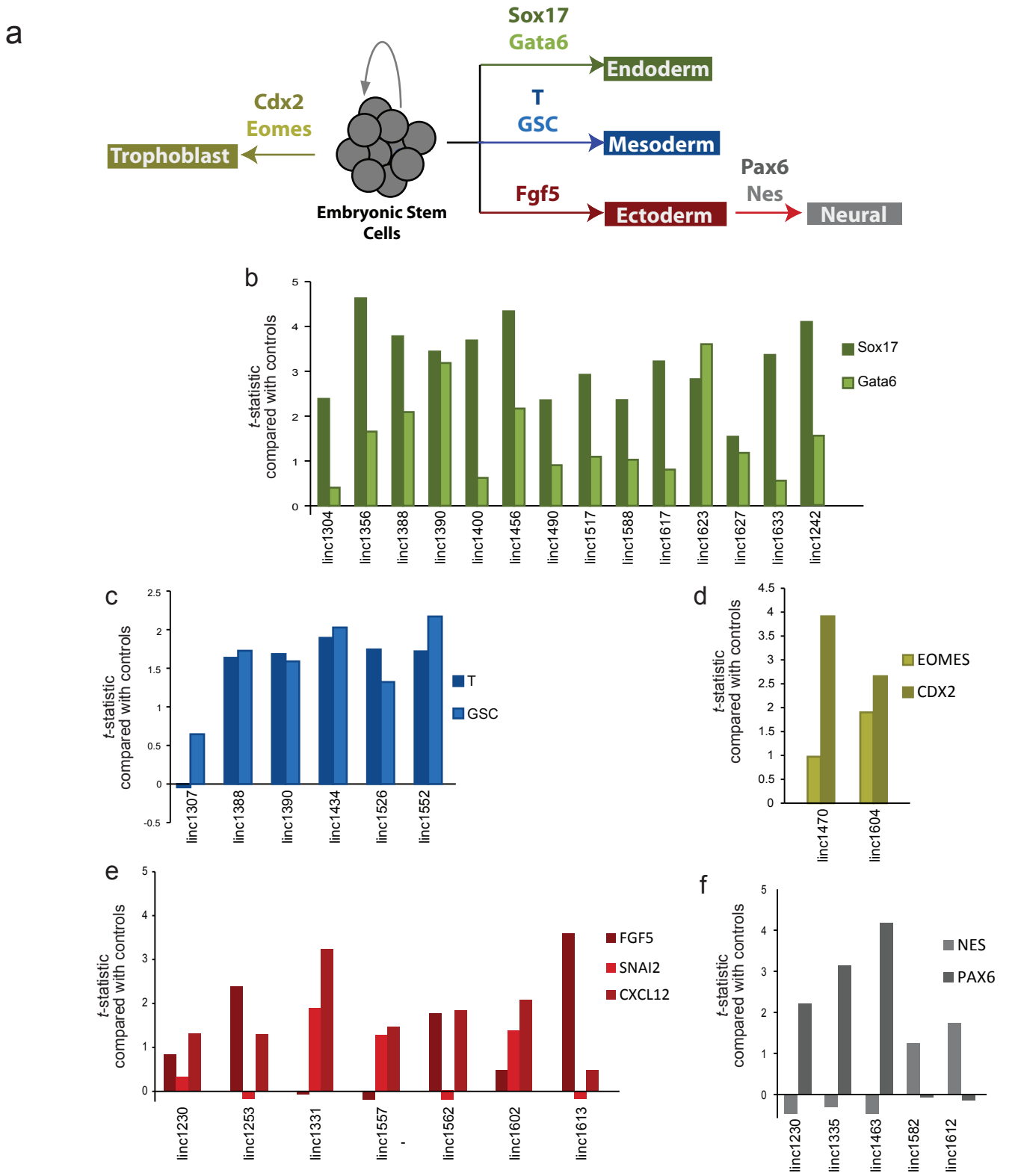

Supplemental Figure 8. Lineage marker gene expression changes upon knockdown of lincRNAs. (a) A schematic of ESC differentiation lineages and well-known marker genes representing each differentiation trajectory are illustrated. (b) Endoderm lineage marker gene Sox17 (dark green) and Gata6 (light green) changes upon lincRNA knockdown are shown for all lincRNAs projected onto the Endoderm state. (c) Mesoderm lineage marker gene T (dark blue) and Gsc (light blue) expression changes upon lincRNA knockdown for all lincRNAs projected onto the Mesoderm state. (d) Trophectoderm lineage marker genes Cdx2 (dark yellow) and Eomes (light yellow) expression changes upon lincRNA knockdown for all lincRNAs projected onto the trophectoderm state. (e) Ectoderm lineage marker genes Fgf5 (dark red), Snai2 (light red), and Cxcl12 (red) expression changes upon lincRNA knockdown for all lincRNAs projected onto the ectoderm state. (f) Neural lineage marker genes Pax6 (dark gray) and Nes (light gray) expression changes upon lincRNA knockdown for all lincRNAs projected onto the neural state. Gene expression changes are displayed in log scale of the t-statistic compared to 27 negative controls.

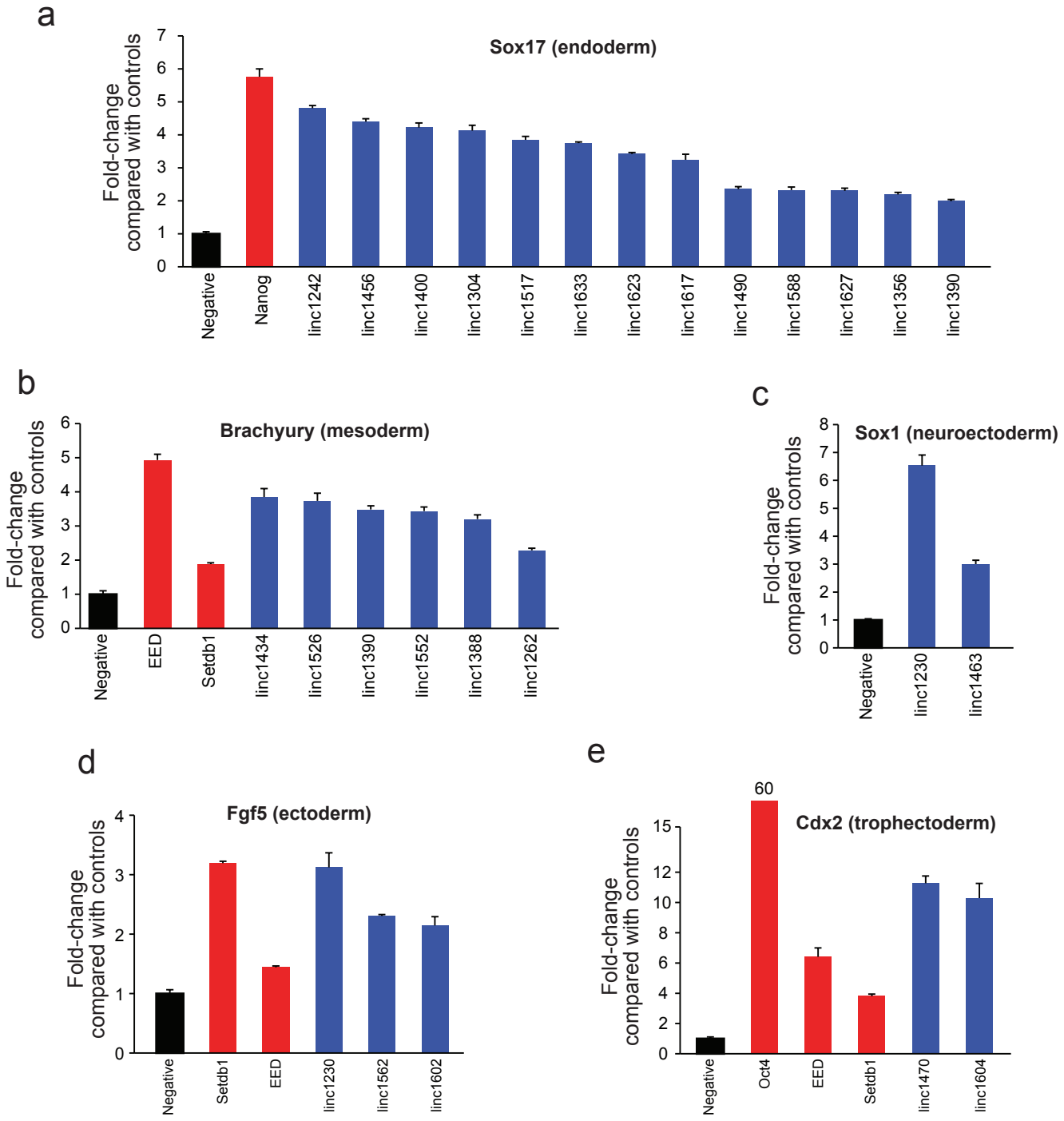

Supplemental Figure 9. qPCR validation of lineage marker gene expression changes upon knockdown of lincRNAs. (a) mRNA expression levels of the Sox17 gene are shown after knockdown with negative control hairpins (black), hairpins targeting Nanog (red), and lincRNAs associated with the Endoderm state (blue). (b) mRNA expression levels of the Brachyury gene are shown after knockdown with negative control hairpins (black), hairpins targeting known protein coding regulators EED and Setdb1 (red), and lincRNAs associated with the Mesoderm state (blue). (c) mRNA expression levels of the Sox1 gene are shown after knockdown with negative control hairpins (black) and lincRNAs associated with the Neuroectoderm state (blue). (d) mRNA expression levels of the Fgf5 gene are shown after knockdown with negative control hairpins (black), hairpins targeting known protein coding regulators Setdb1 and EED (red), and lincRNAs associated with the Ectoderm state (blue). (e) mRNA expression levels of the Cdx2 gene are shown after knockdown with negative control hairpins (black), hairpins targeting known protein coding regulators Oct4, EED, and Setdb1 (red), and lincRNAs associated with the trophectoderm state (blue). All displayed effects are significant ($p<0.0001$) compared to the negative controls.

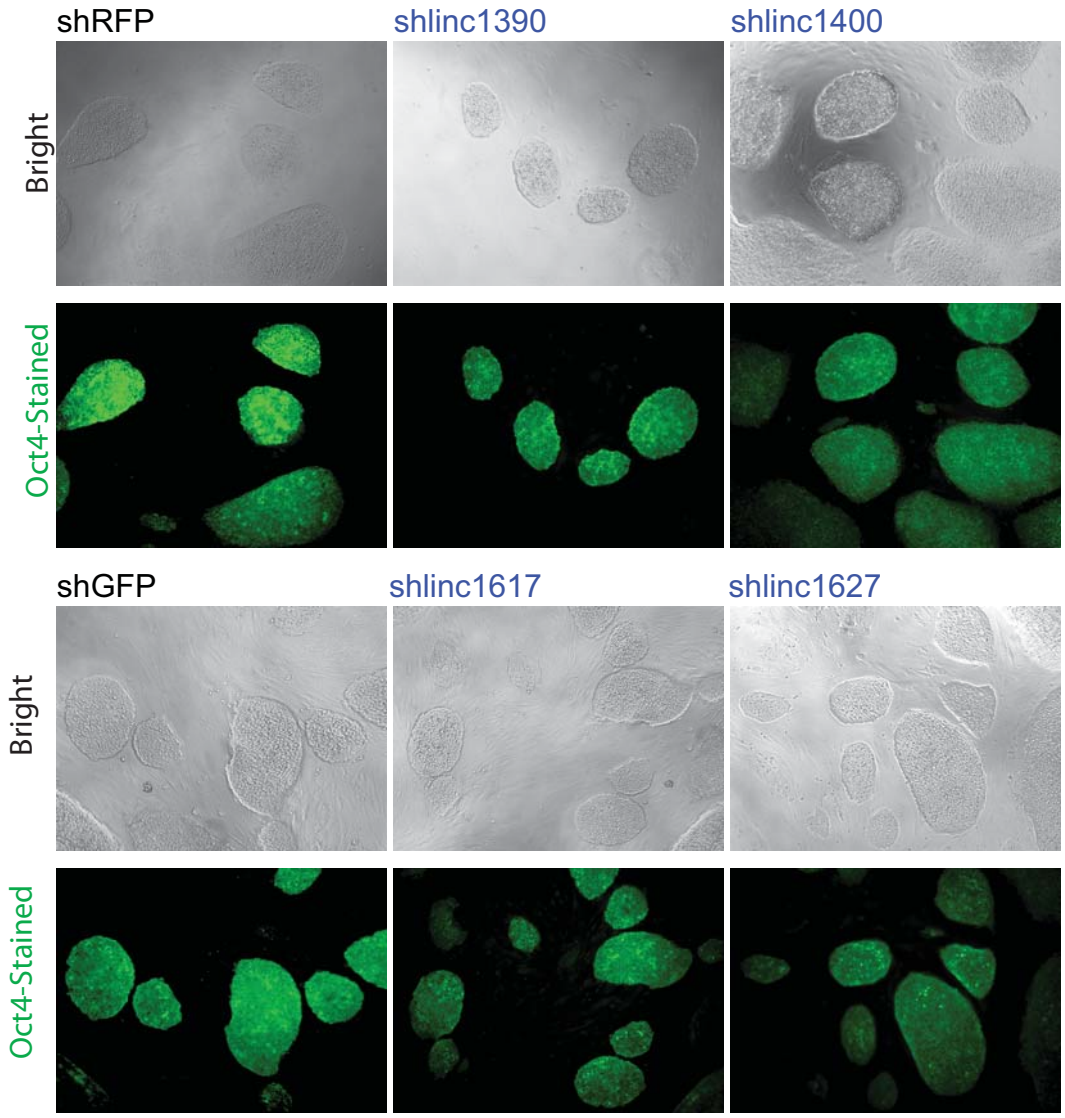

Supplemental Figure 10. Most lincRNAs that upregulate lineage programs upon knockdown do not cause differentiation. Images of ESCs are shown after RNAi knockdowns of lincRNAs associated with upegulation of lineage expression programs. For each panel, a bright-field image is shown (top) and immunofluorescence image of Oct4-stained cells is shown (bottom-green). The first column shows a negative control hairpin targeting RFP and GFP with the remaining columns showing hairpins targeting lincRNA genes (blue labels).

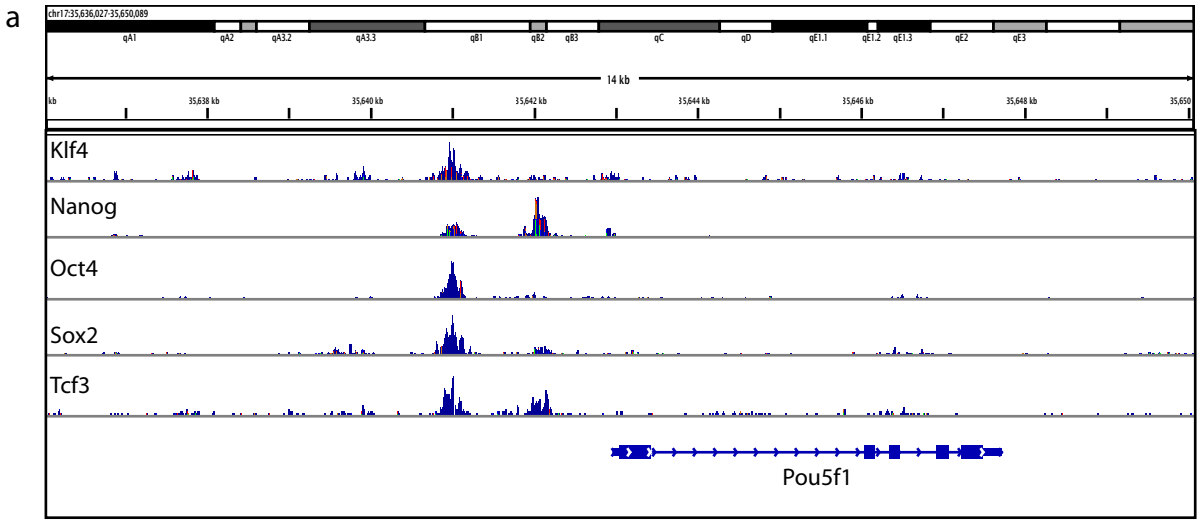

Supplemental Figure 11. Examples of direct transcription factor binding to the promoters of lincRNA genes. Barchart representing transcription factor ChIP-Seq reads mapped to the genomic region surrounding protein-coding and lincRNA promoters. ChIP-Seq reads mapped to the promoter region of (a) Oct4, (b) linc1405, and (c) linc1253.

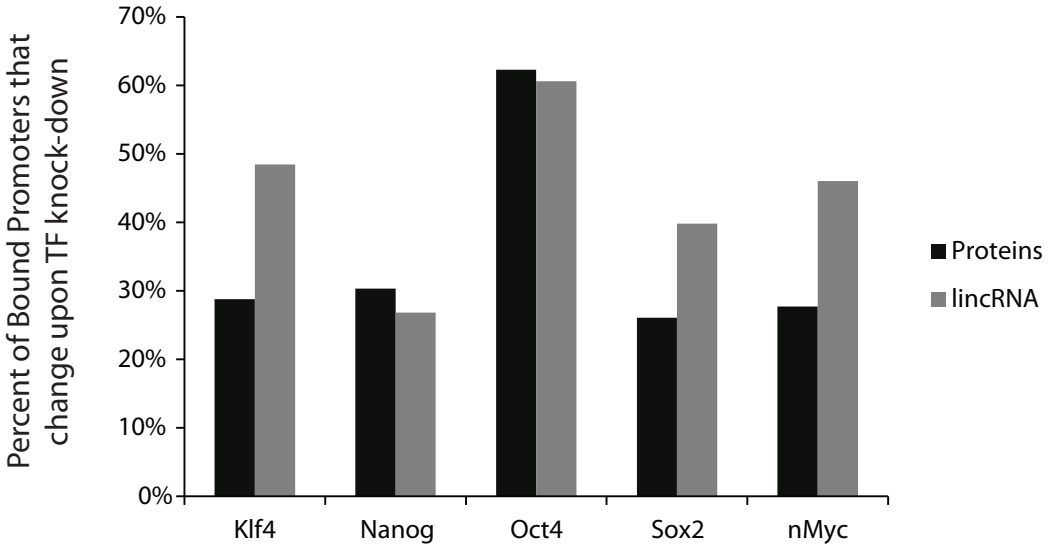

Supplemental Figure 12. Overlap between transcription factor binding and regulation across lincRNA and protein-coding genes. Barchart representing the percent of lincRNAs (grey) and protein-coding (black) promoters that are bound by the indicated transcription factor that also change expression upon knockdown of the transcription factor gene.

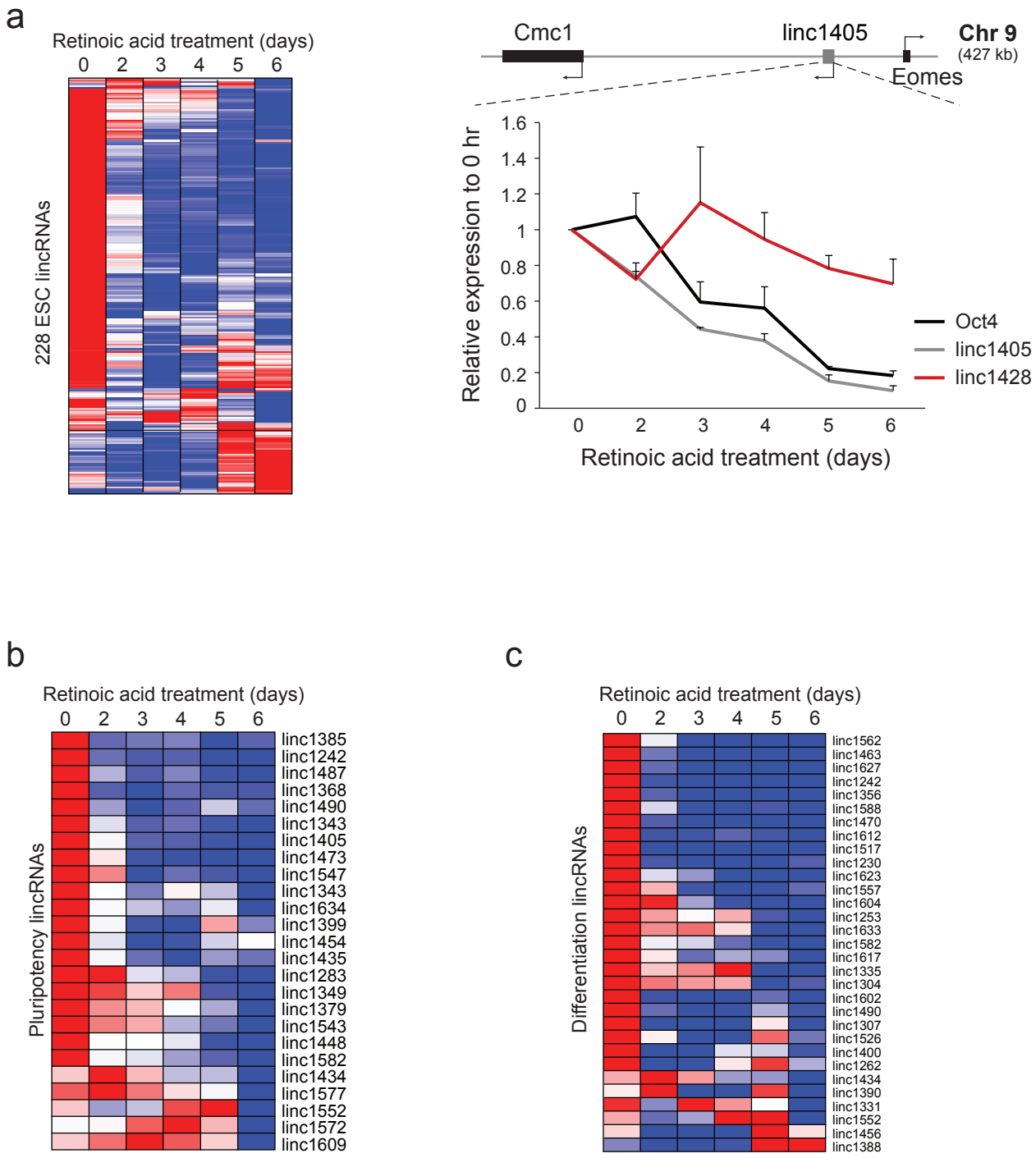

Supplemental Figure 13. lincRNA expression changes upon retinoic acid (RA)-induced differentiation. (a) Expression of lincRNA genes during retinoic acid (RA)-induced differentiation. Left: A heatmap showing expression levels for lincRNAs (rows) across RA time points (columns). Right: Changes in expression levels of Oct4 (black), linc1405 (gray), and linc1428 (red) across time points. (b) A heatmap showing the expression changes for the 26 pluripotency associated lincRNAs across a 6 day RA differentiation time course. (b) A heatmap showing the expression changes for the 31 differentiation associated lincRNAs across the 6 day RA differentiation time course.

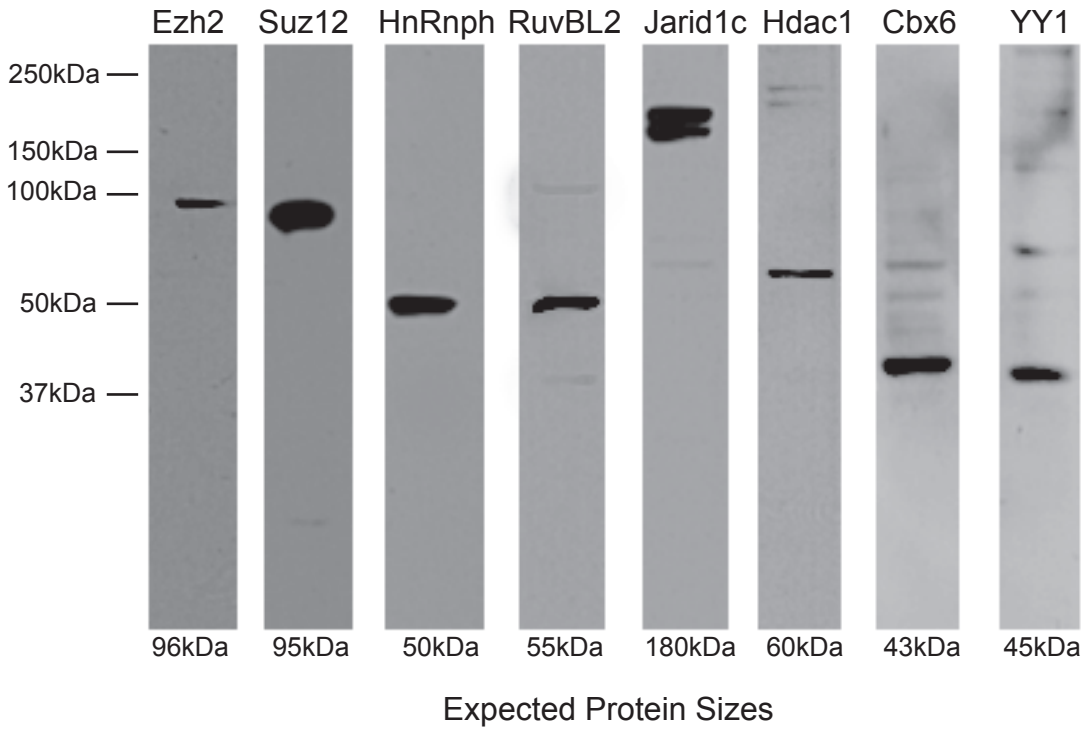

Supplemental Figure 14. Western blot validation of antibodies used for RNA Immunoprecipitation. Western blots are shown for selected successful antibodies used for RNA immunoprecipitation experiments. The protein sizes are indicated on the left, and the expected sizes for each protein is shown below the blot.

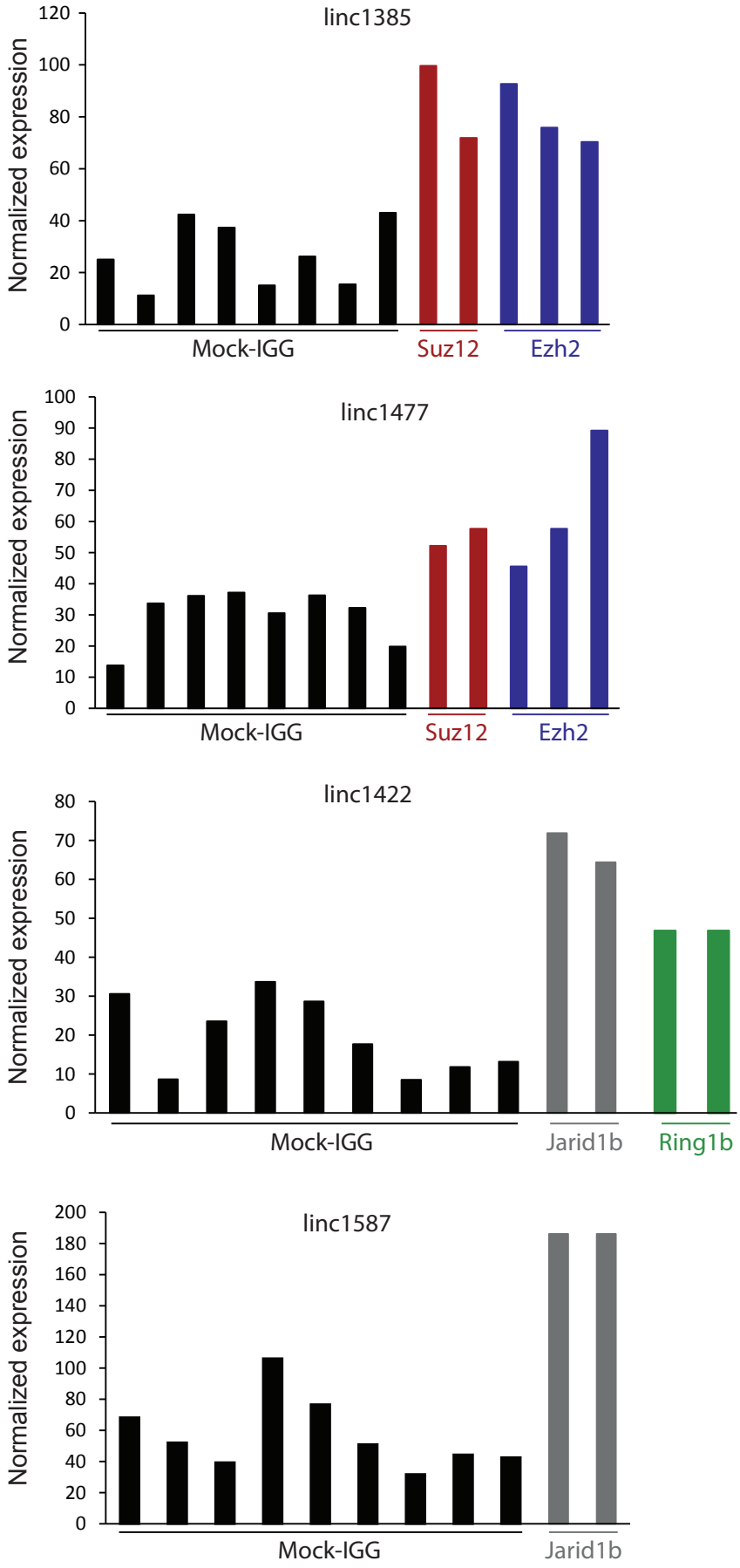

Supplemental Figure 15. Examples of lincRNAs enriched for the chromatin complex binding. The normalized expression levels are shown for 8 mock-IgG controls (black) and replicate chromatin protein immunoprecipitations (Suz12-red, Ezh2-blue, Jarid1b-gray, and Ring1b-green) for 4 selected lincRNA transcripts.

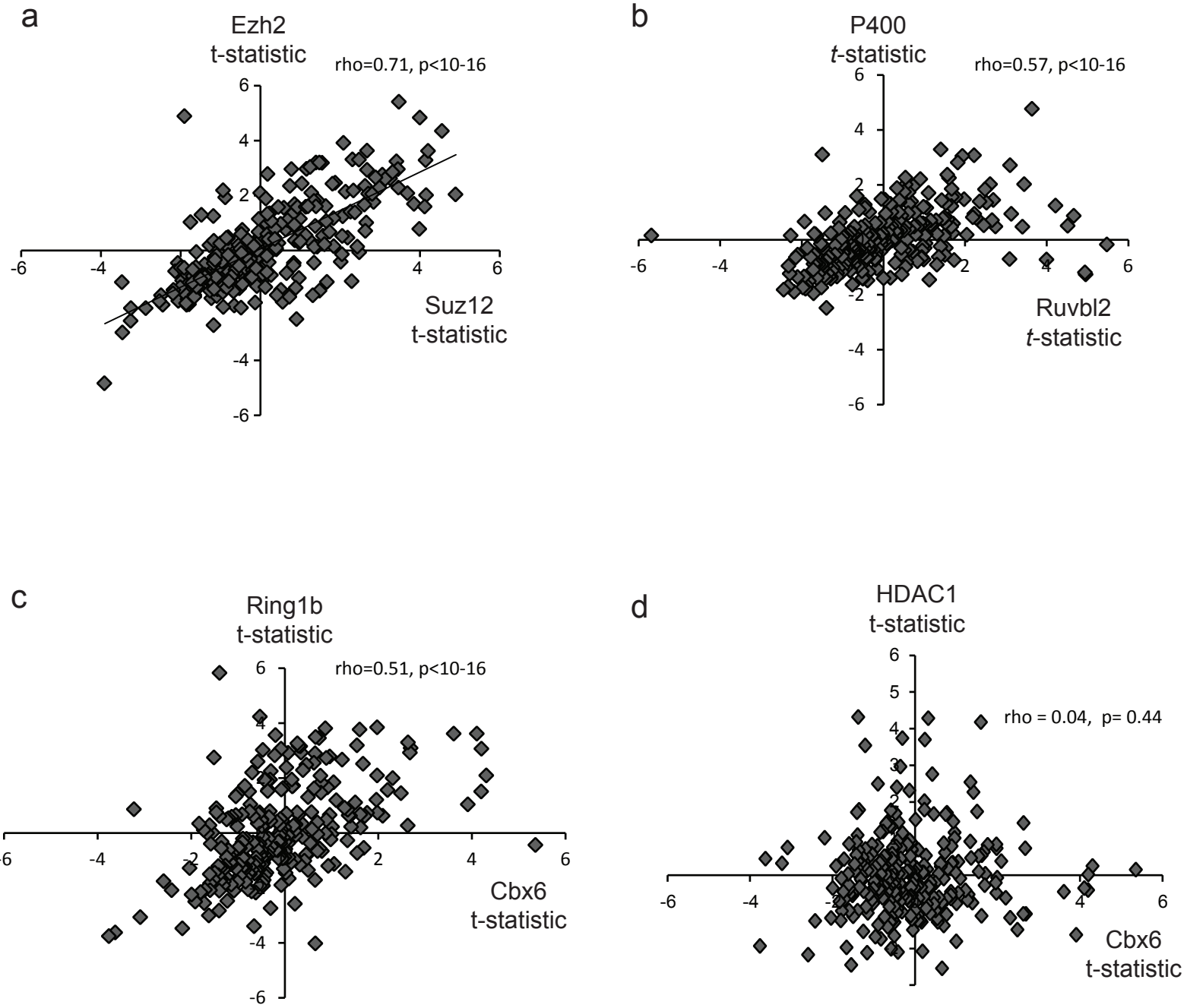

Supplemental Figure 16. Correlation of binding identified upon immunoprecipitation with antibodies to distinct proteins within the same complex. (a) A scatter plot of the t-statistics for enrichment for lincRNAs associated with the PRC2 complex members Ezh2 and Suz12. (b) Scatter plot of the t-statistic for immunoprecipitation of the Tip60/P400 complex members P400 and Ruvbl2. (c) Scatter plot of the t-statistic for immunoprecipitation of the PRC1 complex members Ring1b and Cbx6. (d) Scatter plot of the t-statistic for immunoprecipitation of the unrelated proteins Cbx6 and HDAC1. The Spearman correlation coefficient (rho) and the associated p-value is shown above each plot.

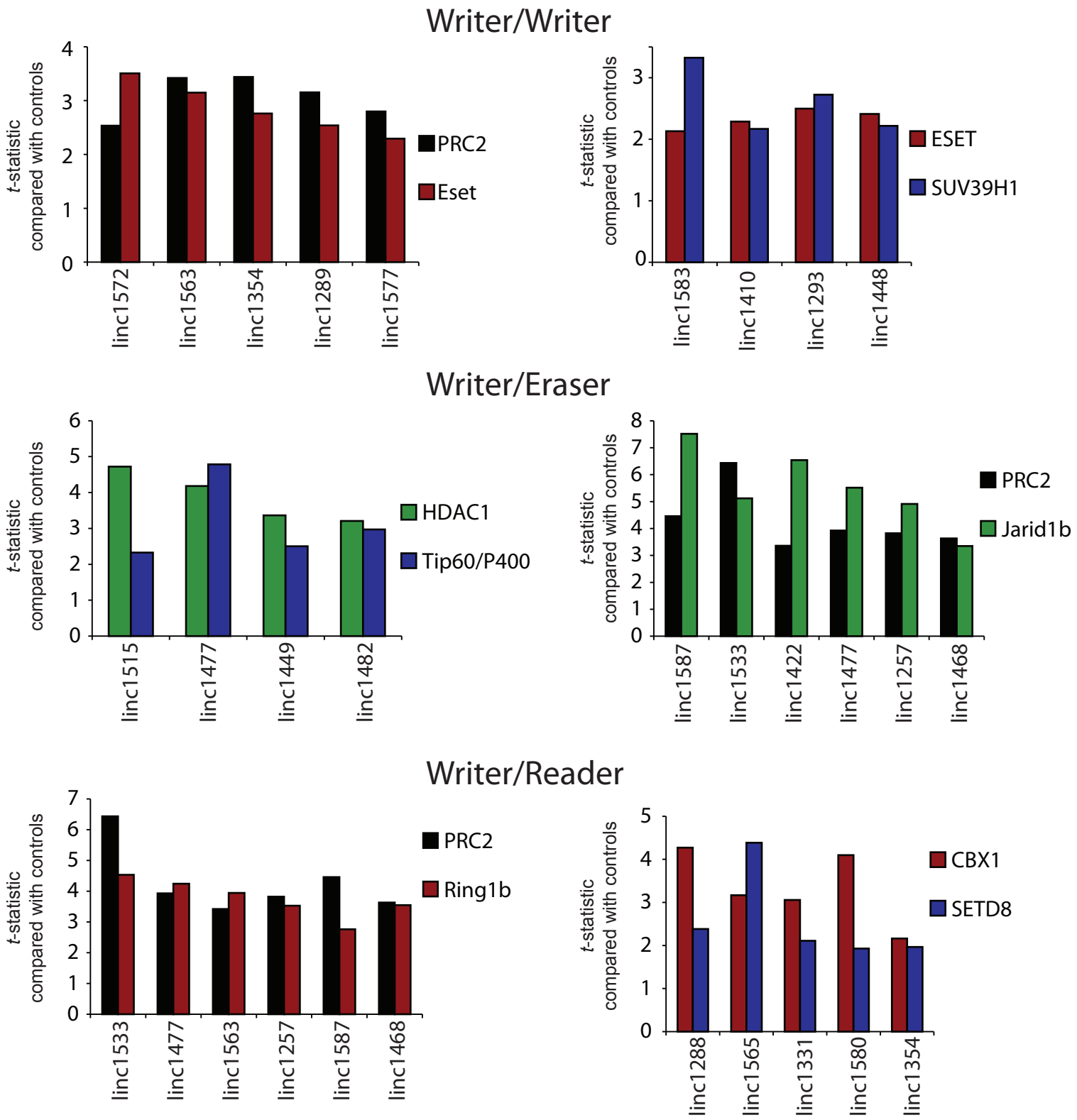

Supplemental Figure 17. Examples of lincRNAs enriched for multiple 'reader', 'writer', and 'eraser' chromatin complexes. Three classes of examples are highlighted, lincRNAs that are enriched for 2 chromatin writer complexes (Writer/Writer), lincRNAs enriched for a chromatin 'writer' and 'eraser' (Writer/Eraser), and lincRNAs enriched for a chromatin 'writer' and 'reader' (Writer/Readers). Enrichment levels are shown as a t-statistic compared to 8 mock-IgG controls.